Experimental validation of a decentralized control law for multi-vehicle collective motion

Daniele Benedettelli, Nicola Ceccarelli, Andrea Garulli, Antonio Giannitrapani

***Abstract*— The paper presents the results of experimental tests carried out to validate the performance of a decentralized control law, for the collective circular motion of a team of nonholonomic vehicles. The considered control strategy ensures global asymptotic stability in the single-vehicle case and local asymptotic stability in the multi-vehicle scenario. The main purpose of this work is to verify these theoretical properties in a real-world scenario. As a side contribution, a low-cost experimental setup is presented, based on the LEGO Mindstorms technology. The setup features good scalability, it is versatile enough to be adopted for the evaluation of different control strategies, and it exhibits several issues to be faced in real-world applications.**

I. Introduction

Recent years have witnessed a growing interest toward multi-agent systems, due to their potential application in many different fields: collective motion of autonomous vehicles, exploration of unknown environments, surveillance, distributed sensor networks, biology, etc. (see e.g. [1], [2] and references therein). Although a rigorous stability analysis of multi-agent systems is generally a very difficult task, nice theoretical results have been obtained both in the case of linear models ([1], [3], [4]) and in the more challenging scenario of nonholonomic vehicles ([2], [5], [6]). On the other hand, most of the proposed algorithms have been tested only in simulation and relatively few experimental results can be found in the literature (see e.g. [7], [8], [9]).

The contribution of the paper is twofold. First, it presents results on the experimental validation of a recently proposed decentralized control law, for the collective circular motion of a group of agents [10]. The objective of the team is to achieve counterclockwise rotation about a reference beacon. The considered control strategy ensures global asymptotic stability in the single-vehicle case and local asymptotic stability in the multi-vehicle scenario. As a second contribution, the paper describes a low-cost experimental setup, based on the LEGO Mindstorms technology, which can be of interest for the performance evaluation of different control schemes for collective motion of multi-vehicle systems. The adopted technology exhibits some severe limitations, in terms of computing power, communication resources and actuator precision, thus making the collective motion problem even more challenging.

The paper is structured as follows. In Section II the collective circular motion problem, for a team of unicycle-like vehicles is stated. Section III summarizes some theoretical properties of the decentralized control law to be validated. Section IV presents an overview of the experimental setup used to evaluate the performance of the proposed control strategy. Experimental results are reported in Section V, while in Section VI some conclusions are drawn.

D. Benedettelli, N. Ceccarelli, A. Garulli and A. Giannitrapani are with the Dipartimento di Ingegneria dell'Informazione, Università di Siena. benedettelli@student.unisi.it, {ceccarelli,garulli,giannitrapani}@dii.unisi.it

II. Problem formulation

Let us consider a group of n agents whose motion is described by the kinematic equations

$$\begin{aligned} \dot{x}_i &= v\cos\theta_i \\ \dot{y}_i &= v\sin\theta_i \qquad\qquad i=1,\dots,n \\ \dot{\theta}_i &= u_i, \end{aligned} \tag{1}$$

where $[x_i \;\; y_i \;\; \theta_i] \in \mathbb{R}^2 \times [-\pi, \pi)$ represents the i-th agent pose, v is the forward speed (assumed to be constant) and u_i is the angular speed, which plays the role of control input for vehicle i. Each vehicle is supposed to be equipped with a sensory system providing range and bearing measurements with respect to: i) a virtual reference beacon, and ii) all its neighbors. Specifically, with reference to the i-th agent, $(\rho_i, \; \gamma_i)$ will denote the measurements with respect to the beacon, while $(\rho_{ij}, \; \gamma_{ij})$ will denote the measurement with respect to the j-th agent (see Figure 1).

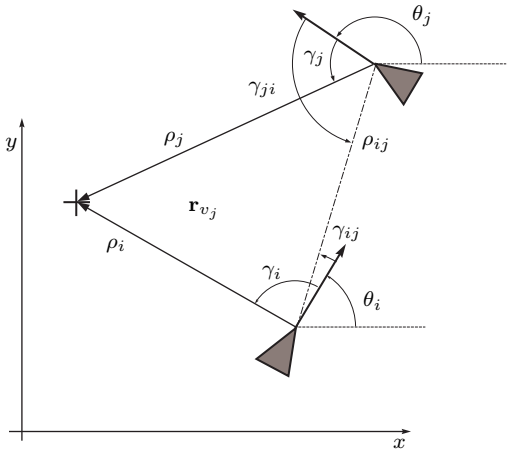

Fig. 1. Two vehicles (triangles) and a beacon (cross).

In order to explicitly take into account sensor limitations, a *visibility region* $\mathcal{V}_i$ is defined for each agent, representing the region where it is assumed that the sensors of the i-th vehicle can perceive its neighbors. In this paper, the visibility

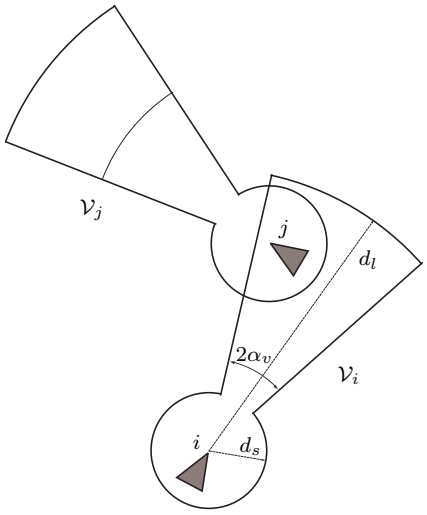

Fig. 2. Visibility region of i-th and j-th vehicle.

region has been chosen as the union of two sets (see Figure 2):

- A circular sector of radius d_l and angular amplitude $2\alpha_v$, centered at the vehicle. It models the presence of a long range sensor with limited angular visibility (e.g., a laser range finder).
- A circular region around the vehicle of radius d_s, which models a proximity sensor (e.g., a ring of sonars) and plays the role of a "safety region" around the vehicle.

This means that the measurements $(\rho_{ij},\ \gamma_{ij})$ are available to the i-th agent if and only if one of the following conditions is verified: (i) $|\rho_{ij}| \leq d_l$ and $|\beta_d(\gamma_{ij})| \leq \alpha_v$; (ii) $|\rho_{ij}| \leq d_s$, where

$$\beta_d(\gamma_{ij}) = \begin{cases} \gamma_{ij} & \text{if } \ 0 \leq \gamma_{ij} \leq \pi \\ \gamma_{ij} - 2\pi & \text{if } \ \pi < \gamma_{ij} < 2\pi. \end{cases} \tag{2}$$

The objective is to design the control inputs u_i so that all the agents achieve circular motion around the beacon, with prescribed radius of rotation and distances between neighbors, while at the same time avoiding collisions. In the next section, a decentralized control law addressing this problem is briefly described (see [10]).

III. Decentralized control law

In order to illustrate the considered control law, some definitions are in order. Let $\mathcal{N}_i$ be the set containing the indexes of the vehicles that lie inside the visibility region $\mathcal{V}_i$ of the i-th agent. Define the functions

$$g(\rho; c, \varrho) = \ln\Big(\frac{(c-1)\cdot\rho + \varrho}{c\cdot\varrho}\Big)$$

and

$$\alpha_d(\gamma;\psi) = \begin{cases} \gamma(t) & \text{if } 0 \leq \gamma(t) \leq \psi \\ \gamma(t) - 2\pi & \text{if } \psi < \gamma(t) < 2\pi. \end{cases}$$

where c, ϱ and $\psi \in (\frac{3}{2}\pi, 2\pi)$ are given constants.

The proposed control law computes the input $u_i(t)$ as

$$u_i(t) = f_{ib}(\rho_i, \gamma_i) + \sum_{\substack{j \neq i \\ j \in \mathcal{N}_i(t)}} f_{ij}(\rho_{ij}, \gamma_{ij}). \tag{3}$$

where

$$f_{ib}(\rho_i, \gamma_i) = \begin{cases} k_b \cdot g(\rho_i; c_b, \rho_0) \cdot \alpha_d(\gamma_i; \psi) & \text{if } \ \rho_i > 0 \\ 0 & \text{if } \ \rho_i = 0, \end{cases} \tag{4}$$

and

$$f_{ij}(\rho_{ij}, \gamma_{ij}) = \begin{cases} k_v \cdot g(\rho_{ij}; c_v, d_0) \cdot \beta_d(\gamma_{ij}) & \text{if } \ \rho_{ij} > 0 \\ 0 & \text{if } \ \rho_{ij} = 0, \end{cases} \tag{5}$$

The function $\beta_d(\gamma_{ij})$ has been defined in (2) while $k_b > 0$, $c_b > 1$, $\rho_0 > 0$, $k_v > 0$, $c_v > 1$, $d_0 > 0$ are the controller parameters. In particular, d_0 is the desired distance between two consecutive vehicles when rotating about the beacon.

The motivation for the control law (3)-(5) relies in the fact that each agent i is driven by the term $f_{ib}(\cdot)$ towards the counterclockwise circular motion about the beacon, while the terms $f_{ij}(\cdot)$ have a twofold aim: to enforce $\rho_{ij} = d_0$ for all the agents $j \in \mathcal{N}_i$ and, at the same time, to favor collision-free trajectories. Indeed, the i-th vehicle is attracted by any vehicle $j \in \mathcal{N}_i$ if $\rho_{ij} > d_0$, and repulsed if $\rho_{ij} < d_0$. Moreover, the term $g(\rho_{ij}, c_v, d_0)$ in (5) is always negative for $\rho_{ij} < d_s$, thus pushing the j-th agent outside the circular safety region around the i-th vehicle and therefore hindering collisions among the vehicles. The aim of such combined actions is to make the agents safely reach the counterclockwise circular motion, with distance d_0 between consecutive vehicles. Notice that the sets $\mathcal{N}_i$ are time-varying, which implies that the control law (3) switches every time a vehicle enters into or exits from the region $\mathcal{V}_i$.

Some theoretical results have been proved for this control law (see [10], [11]). The first one concerns the single-vehicle case, and can be summarized as follows.

Result 1: Let $n = 1$. If the control parameters k_b, c_b, ρ_0 are chosen such that

$$\min_{\rho}\ \rho\, g(\rho; c_b, \rho_0)\ >\ -\frac{2\,v}{3\,\pi\,k_b}, \tag{6}$$

then the counterclockwise rotation about the beacon with rotational radius ρ_e defined as the unique solution of

$$\frac{v}{\rho_e} - k_b \cdot g(\rho_e; c_b, \rho_0) \cdot \frac{\pi}{2} = 0$$

and angular velocity $\frac{v}{\rho_e}$, is a globally asymptotically stable limit cycle for the system (1) with the control law (3).
The above result basically states that in the single-vehicle case, the control law $u_i = f_{ib}$ results in the counterclockwise rotation of the vehicle about the beacon, with a radius ρ_e, for every initial configuration.

For the multi-vehicle case, a sufficient condition has been derived which guarantees the local asymptotic stability of the team configurations corresponding to the collective circular motion about the beacon.

Result 2: Let $\alpha_v \leq \frac{\pi}{2}$, and assume that (6) holds. If the controller parameters satisfy $d_s < d_0 < d_l$ and

$$\frac{\varphi}{2} < \arcsin\left(\frac{d_0}{2\rho_e}\right) < \min\left\{\frac{\pi-\varphi}{n-1}, \alpha_v\right\} \tag{7}$$

where[1]

$$\varphi = \min\left\{\alpha_v\,,\, \arcsin\left(\frac{d_l}{2\rho_e}\right)\right\}$$

then every configuration of n vehicles in counterclockwise circular motion around a fixed beacon, with rotational radius $\rho_i = \rho_e$ defined in (7), $\gamma_i = \frac{\pi}{2}$ and $\rho_{ij} = d_0\ \forall i = 1 \ldots n$ and $\forall j \in \mathcal{N}_i$, corresponds to a limit cycle for the system (1) with the control law (3). Moreover, if

$$\frac{k_v}{k_b} \leq 2\,\frac{c_v}{c_b}\,\frac{c_b - 1}{c_v - 1}, \tag{8}$$

then the aforementioned limit cycles are locally asymptotically stable.

The right side inequality in (7) guarantees that the n vehicles can lie on a circle of radius ρ_e, with distance d_0 between two consecutive vehicles and with at least one vehicle that does not perceive any other vehicle. The left side inequality in (7) ensures that at equilibrium, a vehicle cannot perceive more than one vehicle within its visibility region (see Figure 3), i.e. card$(\mathcal{N}_i) \in \{0, 1\}$. In (7), φ represents the maximum angular distance γ_{ij} such that the i-th vehicle perceives the j-th one, when the two vehicles are moving in circular motion with rotational radius ρ_e.

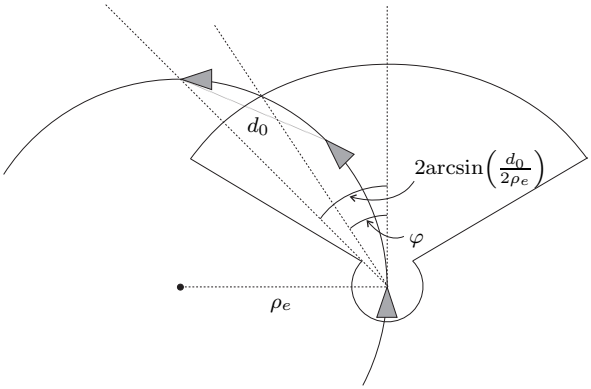

Fig. 3. Three vehicles in an equilibrium configuration satisfying condition (7). Notice that in this example $\varphi = \arcsin\left(\frac{d_l}{2\rho_e}\right)$.

When (7) is satisfied, there can be several different equilibrium configurations, all corresponding to collective circular motion about the beacon. Indeed, there may be q vehicles with card$(\mathcal{N}_i) = 0$ and $n-q$ vehicles with card$(\mathcal{N}_i) = 1$, i.e. the equilibrium configuration is made of q separate platoons. The limit cases are obviously $q = 1$ (a unique platoon) and $q = n$ (n vehicles rotating independently about the beacon).

It is worth noticing that this control law does not require exteroceptive orientation measurements, nor labeling of the vehicles. Each agent can easily compute its control input from range and bearing measurements, without any exchange of information.

Selection of the control law parameters so that the constraints (6),(7) and (8) are satisfied, is always feasible. A detailed discussion on the control parameter design is reported in[11].

[1]With a slight abuse of notation, it is meant that $\varphi = \alpha_v$ whenever $d_l > 2\rho_e$.

IV. Experimental setup

In this section the structure of the mobile robot team used in the experiments will be briefly discussed. A Lego Mindstorms [12] mobile robot team has been built: the robots are identical, except for the LED markers position on robots top, that allow a Centralized Supervision System (CSS) to detect their unique identity, and estimate their position and orientation.

The robots have a differential drive kinematics and are driven by two motors, while an idler wheel acts as third support (see Figure 4). Hence, they are nonholonomic vehicles that can be modelled as unicycles according to (1) and can be driven by setting the linear speed v and the angular speed u. The motors drive the wheels with a 9:1 gear ratio, while the encoders are coupled to the motors with a 1:5 gear ratio: in this way we get enough torque for the driving wheels and a good resolution for encoders (720 ticks per wheel revolution).

Fig. 4. Mindstorms mobile team.

Every vehicle is controlled by a Lego RCX programmable brick [13] equipped with a 16-bit 10Mhz H8/3292 Hitachi processor. The BrickOS realtime operating system [14] allows one to run C/C++ programs to control the motors with 255 PWM levels, to read sensors and to communicate with the CSS via an IR serial protocol. BrickOS also defines its own wireless communication protocol called LNP (LegOS Network Protocol [15]).

The RCX uses incremental encoders for wheel speed control. A two degrees of freedom closed loop controller is implemented to ensure fast and accurate tracking of the linear and angular speed provided by the CSS. A PI feedback control is integrated with a feed-forward action based on the knowledge of the estimated characteristic between RCX PWM output and wheel angular speed. Due to RCX numerical approximations and mechanical dead zones, the vehicles cannot have an angular speed less than $0.05\,rad/s$. The maximum linear speed is about $0.07\,m/s$.

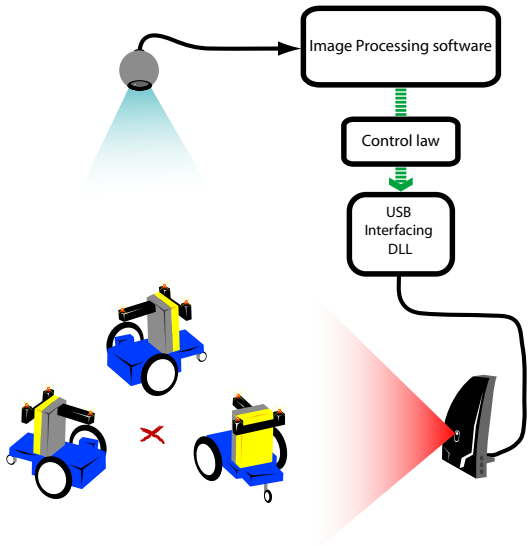

Fig. 5. Centralized Supervision System.

The Centralized Supervision System is illustrated in Figure 5. A camera fixed on the lab ceiling is used to capture the motion of the vehicles. Robots are detected in position, orientation and unique identity thanks to LED lighting markers mounted facing the camera in a isosceles triangle shape. Image capture and processing, and control law implementation are carried out in MATLAB environment, which also sends speed commands to the team via an IR Lego Tower. The IR tower reaches a 10m range and surrounding vertical panels have been used to enhance signal spreading by reflection. To interface MATLAB to a standard Lego USB IR tower a MEX DLL has been written on purpose.

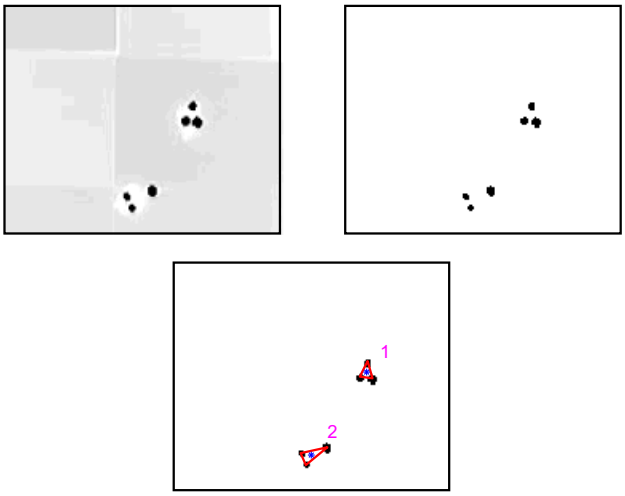

Fig. 6. Image acquisition

Image capturing and processing can be summarized as follows (see Figure 6).

1) A greyscale frame is captured and filtered with a brightness threshold to detect vehicles LED.
2) Robot identity, position and orientation are estimated from the extracted isosceles triangles.
3) Since the Lego robots do not have on-board range finders, range and bearing measurements ρ_i, γ_i, ρ_{ij} γ_{ij} with respect to the (virtual) reference beacon and the robot neighbors, required by the control law (3), are estimated by the software.

The control law output commands are represented as floating point numbers, and need to be converted to 16 bit integers before being sent in order to keep a good precision for on-robot integer arithmetic calculations. The commands for all the robots are packed together and sent once for every sampling time; at the beginning of the experiment every robot is given an ID number accordingly to its lighting marker shape, so that when the robot receives the packet, it recognizes which chunk contains its own data.

At the beginning of an experiment, the robots are given an ID and placed inside the area framed by the ceiling camera. Then, robots behavior can be stated as follows:

- while no IR packet is incoming the robot remains still;
- when the packet is received, the robot starts to move with speeds set by CSS and regulated by the local 2DOFs controller;
- if no new packet is received within a predefined timeout, the robot stops.

The entire experiment is controlled by a MATLAB script that samples robot trajectories, to allow for successive data analysis. Such a centralized architecture has two main purposes. First, the CSS is used to simulate the presence of onboard sensors, thus allowing for the use of inexpensive vehicles. Secondly, all the computations can be done on a standard PC, without overloading the vehicle RCX, which is exclusively devoted to the motor control. Nonetheless, it must be remarked that the tested control law is actually decentralized. In the experiments, the input of each agent is computed by the CSS on the basis of the sole measurements the agent would have access to, if it was equipped with a proper sensory system. Analogously, as far as the control law is concerned, vehicles need not to be distinguishable. They are labelled only for communication purpose.

V. Experimental results

In this section, results of experimental tests involving different number of vehicles, are reported. The forward speed is set to $v = 0.06\ m/s$. Range and bearing measurements are extracted from the images taken by the ceiling camera, simulating on-board range sensors (e.g., a laser rangefinder or a sonar ring). To account for sensor limited field of view, a visibility region like that presented in Section II is assumed, with $d_l = 1\ m$ and $d_s = 0.3\ m$. The angular width α_v has been set to different values in order to simulate different sensors (see Figure 2).

In a first set of tests featuring two vehicles with $\alpha_v = \pi/2$ (Experiment A), the following controller parameters have been used (see Section III): $\psi = 290°$, $k_b = 0.16$, $\rho_0 = 0.3\ m$, $c_b = 2$, $k_v = 0.3$, $d_0 = 0.6\ m$, $c_v = 2$.

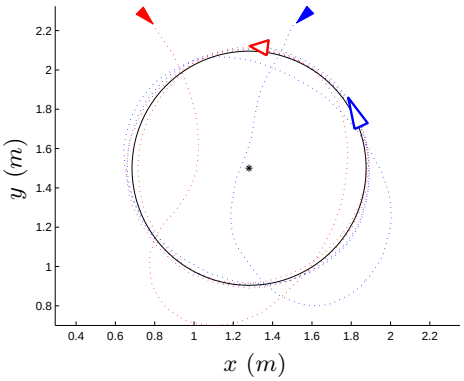

Fig. 7. Experiment A: Vehicle paths (dotted lines) and desired circular path (solid line) about the beacon (asterisk). Filled triangles represent the vehicle initial poses, empty triangles represent the final vehicle poses.

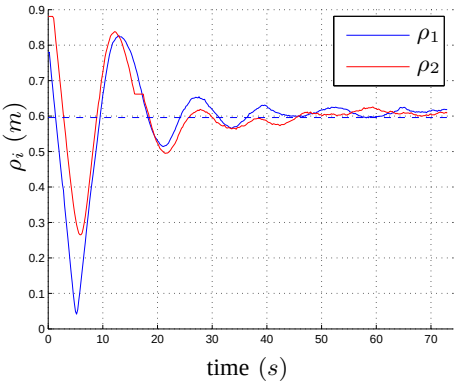

Fig. 8. Experiment A: Actual distances ρ_1, ρ_2 of the vehicles to the beacon (solid lines) and desired radius $\rho_e = 0.6$ (dashed line).

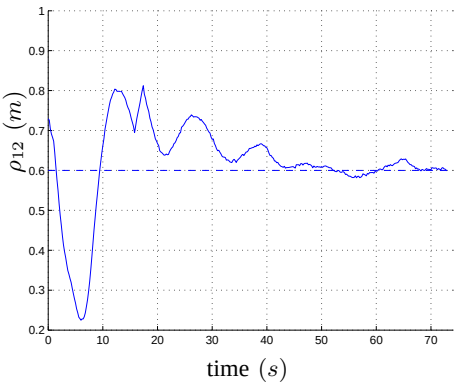

Fig. 9. Experiment A: Actual distance ρ_{12} between the vehicles (solid line) and desired one $d_0 = 0.6$.

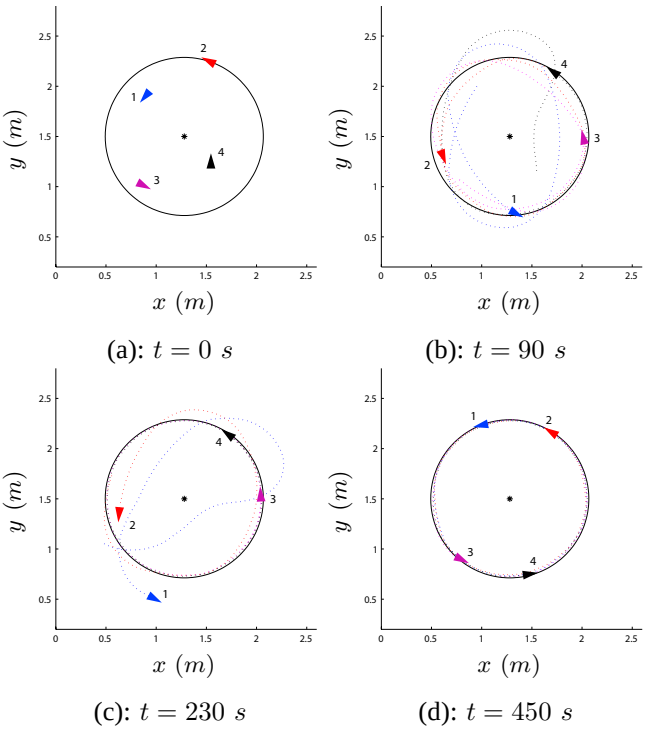

Fig. 10. Experiment B: Team configuration at different time instants. Dotted lines represent vehicle paths during the 90 seconds preceding each snapshot.

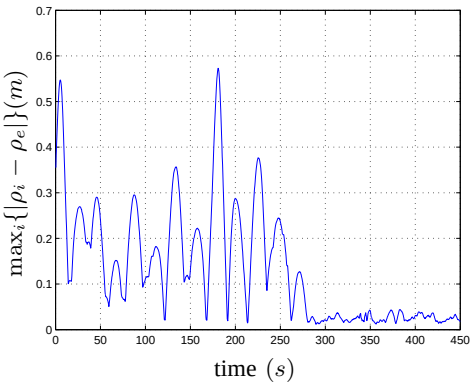

Fig. 11. Experiment B: Maximum deviation $|\rho_i - \rho_e|$ of vehicle distances to the beacon ρ_i, from the desired radius ρ_e.

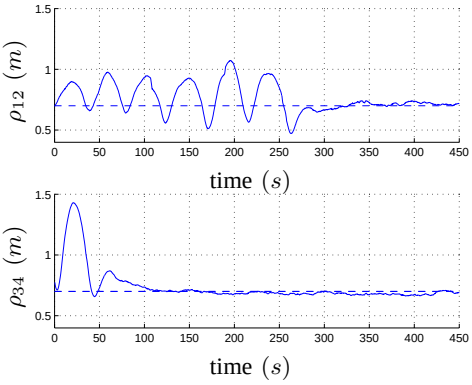

Fig. 12. Experiment B: Actual distances ρ_{12}, ρ_{34} between vehicles belonging to the same platoon (solid line), and desired one $d_0 = 0.7$ (dashed line).

This choice of k_b and ρ_0 corresponds to a desired circular motion of radius $\rho_e = 0.6\ m$, while d_0 models a desired displacement between vehicles in circular motion of $0.6\ m$. The other parameters have been designed such that the right side inequality in (7) is satisfied (the left side inequality can be neglected in the case of two vehicles, since obviously card$(N_i) \in \{0, 1\}$). In Figure 7 the vehicle paths (dotted lines) of a typical experiment are depicted. Filled triangles correspond to the vehicle initial poses, while empty triangles represent the vehicle poses at the end of the run. After a transient (whose duration depends on the initial conditions) both trajectories approach a circle of radius ρ_e, and the vehicle separation settles about d_0. These considerations are supported by Figures 8-9, where the agent distances from the beacon and the inter-vehicle distance are shown, respectively. One can observe that this control strategy is actually effective in avoiding collisions, also when considering the finite size of the vehicles (roughly enclosed in a circle of $0.1\ m$ radius). The effect of the cross terms f_{ij} in the control law (3), and the role of the safety regions around each agent are clearly visible in Figure 7. When the vehicles come too close (see the initial part of the trajectories) the control inputs steer the agents away to prevent collisions.

A second set of experiments has been carried out with four vehicles and $\alpha_v = \pi/4$ (Experiment B). The controller parameters are the same as before, except for $\rho_0 = 0.48\ m$ and $d_0 = 0.7\ m$, resulting in a desired radius $\rho_e = 0.79\ m$. Figure 10 shows four snapshots of the team evolution during a typical run. In this experiment, the vehicles end up in rotating around the beacon in two separate platoons, each one made of two agents. After about 300 seconds, the motion of all the agents stabilizes on the desired circle, as shown in Figure 11. Moreover, the separation between vehicles belonging to the same platoon eventually approaches the desired value d_0. In this case, agents 3 and 4 converge faster to the steady-state, than agents 1 and 2 (see Figure 12).

Several other experiments have been carried out over teams of 3 and 4 vehicles, with different visibility regions, controller parameters and initial vehicle poses. As expected, the final distribution of the robots in separate platoons depends on the initial configuration of the team, while the duration of the transient is mainly influenced by the number of robots in the team.

The overall experimental validation has shown that the considered control law is fairly robust to a number of uncertainty sources and unmodeled effects arising in practice: poorly accurate measurements (due to the low resolution, uncalibrated camera), delays (due to image processing, IR communication between the central unit and vehicle controllers), nonlinear phenomena affecting the actuators (RCX numerical approximations, mechanical dead-zones).

VI. Conclusions

In this paper, the experimental validation of a decentralized control law, for the collective circular motion of nonholonomic vehicles, has been presented. In spite of a quite challenging scenario (inaccurate measurements, communication delays, actuator saturation), promising results have been obtained, suggesting that the considered control strategy can be effectively applied in a real-world scenario. Moreover, the adopted experimental setup provides a cost-effective solution for the validation of different control laws for multi-agent systems.

The enlargement of the experimental area (via multiple cameras) is currently under development. The mobile team will be upgraded using Lego Mindstorms NXT technology, to exploit Bluetooth radio communication and firmware-integrated PID servomotor speed control. Future work will include the validation of collective motion strategies in case of moving reference beacon. In fact, the considered control law has been designed so that smooth transitions between circular and parallel motion are expected when tracking a beacon with time-varying velocity profile [11].

References

[1] A. Jadbabaie, J. Lin, and A. S. Morse. Coordination of groups of mobile autonomous agents using nearest neighbor rules. *IEEE Transactions on Automatic Control*, 48(6):988–1001, June 2003.

[2] J. A. Marshall, M. E. Broucke, and B. A. Francis. Formations of vehicles in cyclic pursuit. *IEEE Transactions on Automatic Control*, 49(11):1963–1974, November 2004.

[3] N. E. Leonard and E. Fiorelli. Virtual leaders, artificial potentials and coordinated control of groups. In *Proceedings of the IEEE Conference on Decision and Control*, pages 2968–2973, Orlando, 2001.

[4] Z. Lin, M. E. Broucke, and B. A. Francis. Local control strategies for groups of mobile autonomous agents. *IEEE Transactions on Automatic Control*, 49(4):622–629, April 2004.

[5] E. W. Justh and P. S. Krishnaprasad. Equilibria and steering laws for planar formations. *Systems and Control Letters*, 52:25–38, 2004.

[6] D. Paley, N. E. Leonard, and R. Sepulchre. Oscillator models and collective motion: Splay state stabilization of self-propelled particles. In *Proceedings of the 44th IEEE Conference on Decision and Control and the 2005 European Control Conference*, pages 3935–3940, Seville, Spain, 2005.

[7] J. A. Marshall, T. Fung, M. E. Broucke, G. M. T. D'Eleuterio, and B. A. Francis. Experiments in multirobot coordination. *Robotics and Autonomous Systems*, (54):265–275, 2006.

[8] A. K. Das, R. Fierro, V. Kumar, J. P. Ostrowski, J. Spletzer, and C. J. Taylor. A vision-based formation control framework. *IEEE Transaction on Robotics and Automation*, 18(5):813–825, October 2002.

[9] Jiangyang Huang, S. M. Farritor, A. Qadi, S. Goddard. Localization and follow-the-leader control of a heterogeneous group of mobile robots. *IEEE/ASME Transactions on Mechatronics*, 11(2):205–215, April 2006.

[10] N. Ceccarelli, M. Di Marco, A. Garulli, and A. Giannitrapani. Collective circular motion of multi-vehicle systems with sensory limitations. In *Proceedings of the 44th IEEE Conference on Decision and Control and European Control Conference ECC 2005*, pages 740–745, Seville, Spain, December 2005.

[11] N. Ceccarelli, M. Di Marco, A. Garulli, and A. Giannitrapani. Collective circular motion of multi-vehicle systems. Technical Report 2007-1, Dipartimento di Ingegneria dell'Informazione, Università di Siena, 2007.
http://www.dii.unisi.it/∼control/MobileRoboticsPage/tr_2007-1.pdf

[12] Lego Mindstorms. http://mindstorms.lego.com/eng/default_ris.asp.

[13] K. Proudfoot. RCX internals.
http://graphics.stanford.edu/∼kekoa/rcx/.

[14] M. L. Noga. BrickOS. http://brickos.sourceforge.net.

[15] M. L. Noga. LNP, LegOS Network Protocol.
http://legos.sourceforge.net/HOWTO/x405.html.